Infection and Drug Resistance

Dovepress
Taylor & Francis Group

Open Access Full Text Article

ORIGINAL RESEARCH

Integrated Single-Cell and Bulk RNA Sequencing Reveals the Diagnostic Value of Synovial Tissue Calprotectin and the MDSC-Associated Immune Microenvironment in Periprosthetic Joint Infection

Ying Tuo[1,*], Yang Xing[2,3,*], Chenghan Chu[2,3], Zhiqing Xiao[4], Puyi Sheng[2,3], Xiaoyu Wu[2,3]

[1]Department of Pathology, The First Affiliated Hospital of Sun Yat-Sen University, Guangzhou, 510080, People's Republic of China; [2]Department of Joint Surgery, The First Affiliated Hospital of Sun Yat-Sen University, Guangzhou, 510080, People's Republic of China; [3]Guangdong Provincial Key Laboratory of Orthopaedics and Traumatology, The First Affiliated Hospital of Sun Yat-Sen University, Guangzhou, 510080, People's Republic of China; [4]Department of Orthopedics, Heyuan Traditional Chinese Medicine Hospital, Heyuan, 517000, People's Republic of China

*These authors contributed equally to this work

Correspondence: Xiaoyu Wu; Puyi Sheng, Email wuxy363@mail.sysu.edu.cn; shengpy@mail.sysu.edu.cn

Infection and Drug Resistance downloaded from https://www.dovepress.com/
For personal use only.

Background: Periprosthetic joint infection (PJI) lacks a universally accepted gold standard for diagnosis, and the immune microenvironment underlying PJI remains incompletely understood. Calprotectin (S100A8/A9) emerged as a key molecule of interest in PJI, yet its expression profile in synovial tissue has not been fully characterized.

Methods: Bulk RNA sequencing was performed on sonication fluid samples from 53 PJI patients and 40 aseptic failure (AF) controls from the GEO database. Differential gene expression, immune cell infiltration, and pathway enrichment analyses were conducted. Single-cell RNA sequencing (scRNA-seq) data from synovial tissue were integrated to characterize the cellular distribution of S100A8 and S100A9 and to investigate immune cell interactions using the CellChat algorithm. Immunohistochemical staining was performed to validate calprotectin expression in synovial tissue.

Results: By integrating bulk and scRNA-seq, we characterized the cellular expression profile of S100A8 and S100A9 within the immune microenvironment of PJI synovial tissue. The results showed that S100A8 and S100A9 were markedly upregulated in PJI synovial tissue and predominantly expressed by myeloid-derived suppressor cells (MDSCs). The enrichment of S100A8/A9-expressing MDSCs in PJI synovial tissue was associated with immune features indicative of an immunosuppressive microenvironment. Cell–cell communication analysis revealed extensive interactions between MDSCs and NK cells as well as macrophages in the PJI microenvironment. Furthermore, immunohistochemical analysis demonstrated significantly elevated calprotectin expression in PJI synovial tissue, and receiver operating characteristic (ROC) curve analysis supported the diagnostic value of synovial tissue calprotectin for PJI.

Conclusion: This study demonstrates that S100A8 and S100A9 are highly expressed in the synovial tissue of patients with PJI and provides additional evidence supporting the diagnostic value of calprotectin in synovial tissue. In addition, we comprehensively characterize the cellular expression profiles of S100A8 and S100A9 in PJI synovial tissues, revealing a close association with MDSC-related immunosuppression.

Keywords: periprosthetic joint infection, calprotectin, biomarker

Introduction

Periprosthetic joint infection (PJI) is one of the most serious complications following total joint arthroplasty (TJA). The reported infection rate after total hip arthroplasty ranges from 0.3% to 1.7%, while for total knee arthroplasty, it is between 0.8% and 1.9%.[1,2]

https://doi.org/10.2147/IDR.S574816
Received: 3 November 2025
Accepted: 19 February 2026
Published: 3 March 2026

© 2026 Tuo et al. This work is published and licensed by Dove Medical Press Limited. The full terms of this license are available at https://www.dovepress.com/terms.php and incorporate the Creative Commons Attribution – Non Commercial (unported, v4.0) License (http://creativecommons.org/licenses/by-nc/4.0/). By accessing the work you hereby accept the Terms. Non-commercial uses of the work are permitted without any further permission from Dove Medical Press Limited, provided the work is properly attributed. For permission for commercial use of this work, please see paragraphs 4.2 and 5 of our Terms (https://www.dovepress.com/terms.php).

Diagnosing PJI is challenging, as there is no established gold standard. Diagnosis of PJI usually relies on a combination of patient symptoms, blood tests, joint fluid analysis, and periprosthetic tissue samples.[3,4] In 2011, the Musculoskeletal Infection Society (MSIS) Working Group proposed major and minor criteria to aid in PJI diagnosis, addressing the lack of a single recognized diagnostic standard.[5] According to the 2018 consensus, major diagnostic criteria comprise (1) a sinus tract connecting to the joint, or (2) identical pathogenic organisms isolated from ≥2 separate periprosthetic tissue cultures. Minor criteria include synovial fluid biomarkers such as C-reactive protein (CRP), alpha-defensin, leukocyte esterase, and synovial fluid hematocrit.[6,7] These criteria indicate that PJI diagnosis cannot rely on a single biomarker but requires a combination of clinical manifestations, blood tests, and synovial biomarkers.

S100A8 and S100A9, members of the S100 family of calcium-binding proteins (also known as migration repressor-related proteins 8 and 14), are primarily expressed in neutrophils and monocytes/macrophages.[8] S100A8 and S100A9 form the heterodimeric calprotectin complex, which exhibits antibacterial properties and has emerged as a promising diagnostic biomarker for PJI.[9–15] Therefore, calprotectin detection may compensate for the reduced sensitivity of traditional cultures in diagnosing infections with low bacterial loads. Meanwhile, Zhang et al[16] and Lazic et al[17] demonstrated that the diagnostic value of calprotectin assay for PJI is superior to that of CRP, ESR, SF-WBCs, and SF-PMNs. Additionally, several individual cohort studies have demonstrated excellent diagnostic accuracy of synovial fluid calprotectin, with high sensitivity and specificity for distinguishing PJI from aseptic failure (AF).[16,18] Calprotectin can be measured using different analytical approaches, including enzyme-linked immunosorbent assays (ELISA) and rapid lateral flow tests, most commonly in synovial fluid samples. These assays have been reported to provide rapid and reliable results, making calprotectin a practical biomarker for clinical application in PJI diagnosis. However, previous studies have primarily focused on calprotectin in synovial fluid as a diagnostic marker for PJI, while the expression patterns of calprotectin in synovial tissue remain insufficiently characterized. In particular, its cellular sources and immunological roles within the PJI synovial immune microenvironment have not been systematically investigated.

In addition to being a diagnostic marker, calprotectin also plays an important role in the immune microenvironment of local tissues. Endogenous calprotectin is known to regulate adaptive immunity by inducing the accumulation of myeloid-derived suppressor cells (MDSCs), which in turn inhibit T-cell responses.[19,20] Sinha et al demonstrated that calprotectin binds to glycoprotein receptors on MDSCs, promoting their recruitment and aggregation in inflamed tissues.[20] Together, these studies provide a biological rationale for investigating the link between calprotectin expression and MDSC-mediated immunosuppression in PJI.

In this study, we conducted an integrated analysis using bulk RNA sequencing (RNA-seq) of sonicate fluid from PJI and AF patients and single-cell RNA sequencing (scRNA-seq) of synovial tissue. Our multi-omics approach was designed to evaluate the diagnostic association between synovial tissue calprotectin and PJI and to explore its potential role within the PJI immune microenvironment. Using scRNA-seq data, we examined the distribution of calprotectin (S100A8/A9) across different immune cell populations in synovial tissues, including immunosuppressive subsets such as MDSCs. Then we used integrated analyses to investigate the association between S100A8/A9 expression and immunosuppressive immune cell subsets and to explore its potential involvement in immunosuppressive immune interactions within the PJI microenvironment. Finally, immunohistochemical (IHC) staining of synovial tissues from patients with PJI and AF was used to assess calprotectin expression levels, and receiver operating characteristic (ROC) curve analysis was performed to evaluate its diagnostic performance in synovial tissues. Overall, this study aims to characterize the profile of calprotectin in PJI and to evaluate its potential utility as a synovial tissue diagnostic biomarker.

Methods

Patients

This study obtained synovial tissues from a total of 100 patients during surgery, which included 45 patients who underwent revision TJA for PJI, 45 patients who underwent revision TJA for AF, and 10 patients who underwent primary TJA for OA. These tissues were subsequently used for IHC staining. The diagnosis of PJI was based on the 2018 Musculoskeletal Infection Society (MSIS) criteria.[21] Patients with inflammatory arthritis, malignancy, systemic autoimmune disease, or incomplete clinical data were excluded from the study. OA patients had no prior history of joint

infection or revision surgery at the time of sample collection. This study was conducted in accordance with the Declaration of Helsinki. Ethical approval was obtained from the Ethics Committee of the First Affiliated Hospital of Sun Yat-sen University (IRB No. [2023]740), and written informed consent was obtained from all patients prior to the commencement of the study.

Samples and Sequencing Methods

We analyzed bulk RNA-sequencing data from implant sonication fluid samples of 93 patients (53 with PJI and 40 with AF; GSE255786). Following cryopreservation at -80°C, total RNA was extracted using the miRNeasy Serum/Plasma Kit (QIAGEN) and sequenced on an Illumina HiSeq 4000 platform (100-cycle paired-end reads, 10 samples/lane).[3]

The osteoarthritis (OA) gene expression dataset (GSE254682) comprised synovial tissues from 8 OA patients undergoing joint surgery and 7 healthy controls from sports injury procedures. All samples underwent pathological confirmation prior to whole transcriptome analysis.[22]

ScRNA-seq data were obtained from synovial tissues of PJI (GSE241739, n=2) and OA (GSE216651, n=5) patients. PJI samples were processed as unsorted single-cell suspensions during revision arthroplasty, with libraries prepared using 10X Genomics Chromium 3' v3.1 kit and sequenced on NovaSeq 6000 (50,000–100,000 reads/cell). OA samples followed comparable processing protocols.[23,24]

Identification of Differentially Expressed Genes (DEGs) in the Synovium of Patients with PJI and AF

We used the "Limma" R package, a specialized tool for analyzing differential gene expression, to identify DEGs between the PJI and AF samples. Raw sequencing reads were aligned to the human reference genome, and gene-level counts were generated and normalized prior to differential expression analysis using the Limma package. Only genes with a P-value < 0.01 and |log2FC| > 1 were selected. The DEGs were visualized through volcano plots and heatmaps generated using the "ggplot2" and "heatmap" packages.

Functional Enrichment Analysis of DEGs

Gene ontology (GO) analysis was conducted to describe the function of genes and proteins, including biological processes (BP), molecular functions (MF), and cellular components (CC). Additionally, we employed the Kyoto encyclopedia of genes and genomes (KEGG) database to explore the biological pathways associated with DEGs. GO and KEGG analyses were performed using the "clusterProfile" package, with significance criteria set at $P < 0.05$.

Immune Cell Infiltration and Correlation with S100A8 and S100A9

Immune cell infiltration and immune functional/pathway activities were quantified using the single-sample gene set enrichment analysis (ssGSEA) algorithm implemented in the R package GSVA. The analysis was based on predefined immune-related gene signatures described by Bindea et al,[25] which include both immune cell–specific signatures (eg, B cells, $CD8^+$ T cells, macrophages) and functional/pathway signatures (eg, T cell co-stimulation, MHC class I, cytolytic activity). We analyzed the correlation between S100A8, S100A9, and immune cells, as well as other genes, using the "corrplot" package. The "Estimate" package was utilized to calculate immune scores for PJI and AF samples. Subgroup comparisons were performed by stratifying samples into high- and low-expression groups for S100A8 and S100A9, based on their respective median expression values.

Analysis of S100A8 and S100A9 in OA and PJI Based on Bulk RNA Sequencing

DEGs between OA and normal samples were identified using the "Limma" package. The expression of S100A8 and S100A9 in both gene expression matrices was analyzed using the "RobustRankAggreg" package.

scRNA-Seq Analysis

Single-cell RNA-seq data were processed and quality-controlled using standard procedures, followed by clustering and visualization of cell populations. Details of filtering thresholds, normalization, and clustering parameters are provided in Supplementary Methods. Differential gene expression in each cluster was identified using the "FindAllMarkers" function, and cell types were annotated using the "SingleR" package.

Cell-to-cell communication at the molecular level was analyzed using the "CellChat" R package, with receptor-ligand pairs counted and visualized.

IHC Staining

IHC staining for calprotectin was performed on synovial tissues, and the positive staining area was quantified using ImageJ software. Detailed staining protocols and image analysis procedures are provided in Supplementary Methods. [26]

Statistical Analysis

Data analysis was conducted using R software (version 4.2.2). Student's *t*-test or Wilcoxon tests were used to assess differences between groups, while Pearson or Spearman correlations were calculated between variables. Statistical significance was set at $P < 0.05$. For transcriptomic analyses, P-values were adjusted for multiple testing using the false discovery rate (FDR) where applicable.

IHC staining data were analyzed using GraphPad Prism (version 8.0). Normality and log-normality tests were performed to determine data distribution. For nonparametric data, descriptive statistics (mean ± SEM) were calculated. The Kruskal–Wallis and Mann–Whitney tests were used to assess statistical significance. ROC curves were generated in GraphPad Prism, and Youden's criteria were applied to calculate biomarker thresholds.

Results

Expression Features of S100A8 and S100A9 and Functional Enrichment Analysis

To investigate whether the transcriptomic landscape of PJI highlights calprotectin (S100A8/S100A9) as a key player, we identified a total of 1150 DEGs, including 928 upregulated and 222 downregulated genes (Figure 1A–C), which were visualized as a volcano plot (Figure 1D) using dataset GSE255786 from the GEO database.

Among DEGs in PJI versus AF samples, S100A8 and S100A9 were among the most highly upregulated, highlighting the central role of calprotectin in the disease (log2 fold change 1.56 and 1.70, Figure 2A and B). GO and KEGG enrichment analyses were performed to identify key pathways and functions associated with the upregulated DEGs in PJI patients. GO analysis showed that DEGs were enriched in BP such as taxis, response to molecules of bacterial origin, and response to lipopolysaccharides. In terms of CC, they were mainly concentrated in protein complexes involved in cell adhesion, protein-lipid complexes, and postsynaptic cytoskeleton. For MF, they were primarily involved in scavenger receptor activity, protein-lipid complex binding, and low-density lipoprotein particle binding (Figure 2C). KEGG analysis indicated that upregulated DEGs were significantly associated with pathways such as viral protein interactions with cytokines and cytokine receptors, Legionellosis, and the TNF signaling pathway (Figure 2D). Furthermore, S100A8 and S100A9 were also upregulated in the IL-17 signaling pathway (Figure 2E), which was highlighted in the KEGG enrichment analysis for PJI-related genes (Figure 2D). The IL-17 pathway is a central regulator of neutrophil recruitment and activation, promoting the expression of pro-inflammatory mediators including calprotectin (S100A8/A9) in neutrophils.[27] This suggests that the elevated S100A8/A9 expression observed in PJI tissues may reflect IL-17–driven neutrophil responses, linking the pathway to both neutrophil biology and local calprotectin production.

To investigate whether S100A8/A9 expression varied according to infective pathogens, PJI samples were stratified into *S. aureus* PJI, *S. epidermidis* PJI, Non-S. aureus/S. epidermidis PJI, and AF.[3] S100A8/A9 expression was significantly higher across all pathogen-defined PJI subgroups compared with AF group. (Figure S1A-B) Consistent with this subgroup analysis, pooled PJI samples also showed significantly elevated S100A8/A9 expression compared with AF group. (Figure 2A) Overall, both S100A8 and S100A9 expression were increased across all PJI subgroups compared with the AF group, regardless of infective species.

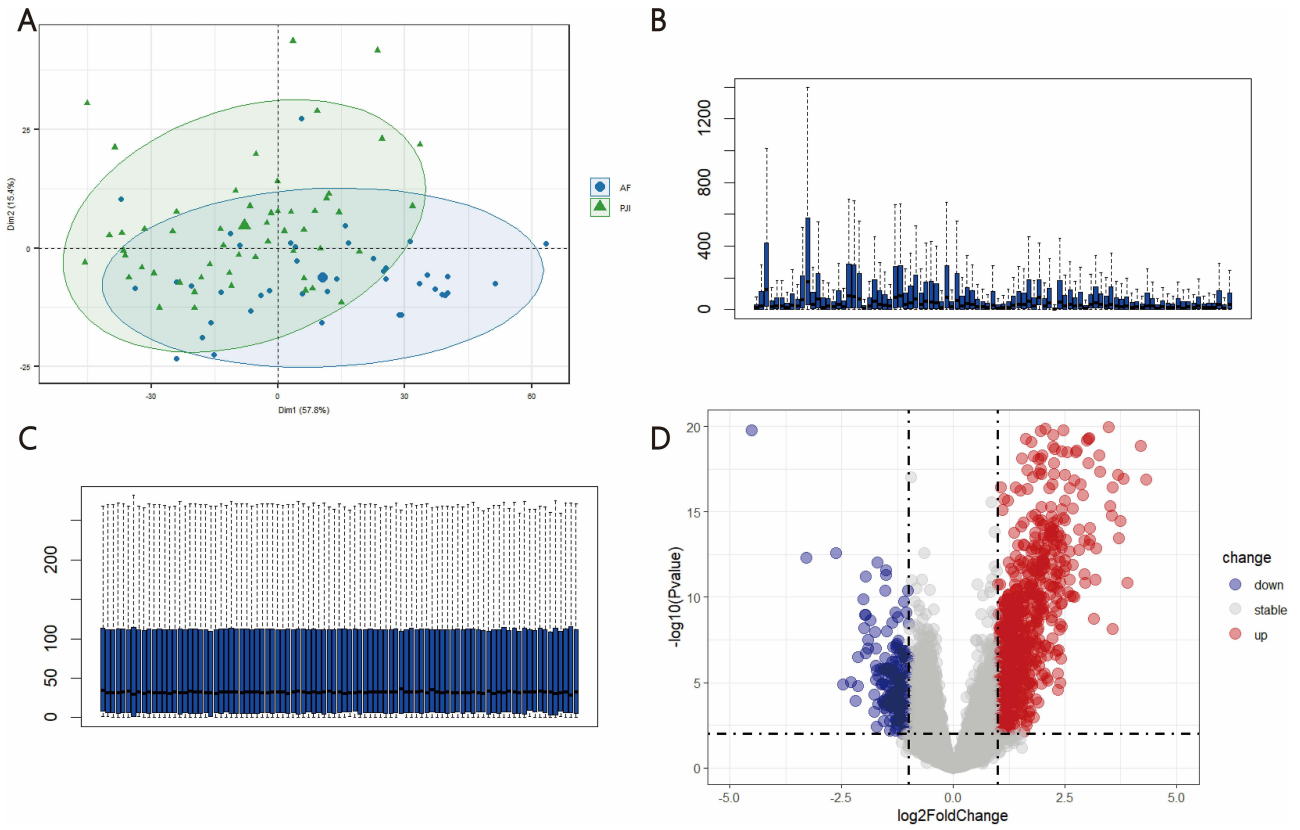

Figure 1 Bulk RNA sequencing data analyses. (**A**) PCA plots showing clustering of samples based on gene expression profiles; total DEGs (**B**) before and (**C**) after normalization; (**D**) analysis of variance volcano plots, where grey represents genes with adj. P. Val > 0.05.

Immune Cell Infiltration and Correlation with S100A8 and S100A9 Expression

To explore the immunological context of calprotectin upregulation, we applied ssGSEA to evaluate immune cell enrichment in PJI synovial tissues compared with AF controls. We observed significantly increased enrichment of five immune signatures in PJI samples, including neutrophils, MDSCs, T cell co-stimulation, Th1 cells, and Tfh cells. In contrast, three signatures—MHC class I, T helper cells, and macrophages—showed significantly decreased enrichment in PJI samples (Figure 3A–C). Notably, MDSCs enrichment scores were significantly higher in PJI patients compared to AF controls (Figure 3C; Wilcoxon test, $p < 0.001$). Moreover, MDSCs enrichment was inversely associated with macrophage abundance across all samples, showing a moderate negative correlation (Spearman's $\rho = -0.53$, $p < 0.001$; Figure 3A), as visualized in the correlation heatmap. These results indicate that increased MDSCs infiltration is associated with reduced macrophage presence in PJI tissues.

Through integrated analysis of two independent datasets, we consistently observed significantly elevated expression of S100A8 and S100A9 in PJI samples compared to aseptic controls (Figure 3E). Building on this observation, we further examined the relationship between S100A8/S100A9 expression and the enrichment of immune cell subsets. A strong positive correlation was observed between S100A8/S100A9 expression and the enrichment scores of MDSCs and neutrophils (Figure 3D), suggesting that S100A8/S100A9 expression in PJI tissues is closely associated with an MDSC-enriched immune landscape, a feature commonly linked to immunosuppressive microenvironments.

Notably, although S100A8 and S100A9 expression was not associated with changes in $CD8^+$ T cell abundance, their elevated expression suggested a potential impact on T cell functional states rather than cell numbers. To further explore the potential immunosuppressive impact of S100A8 and S100A9, we examined their correlations with T cell-associated effector genes. As shown in Figure 3F, both S100A8 and S100A9 expression levels were negatively correlated with multiple cytotoxic and T cell activation–related genes, including IL22, IL2, ICOS, GZMM, CD8A, TBX21, and IFNG.

https://doi.org/10.2147/IDR.S574816

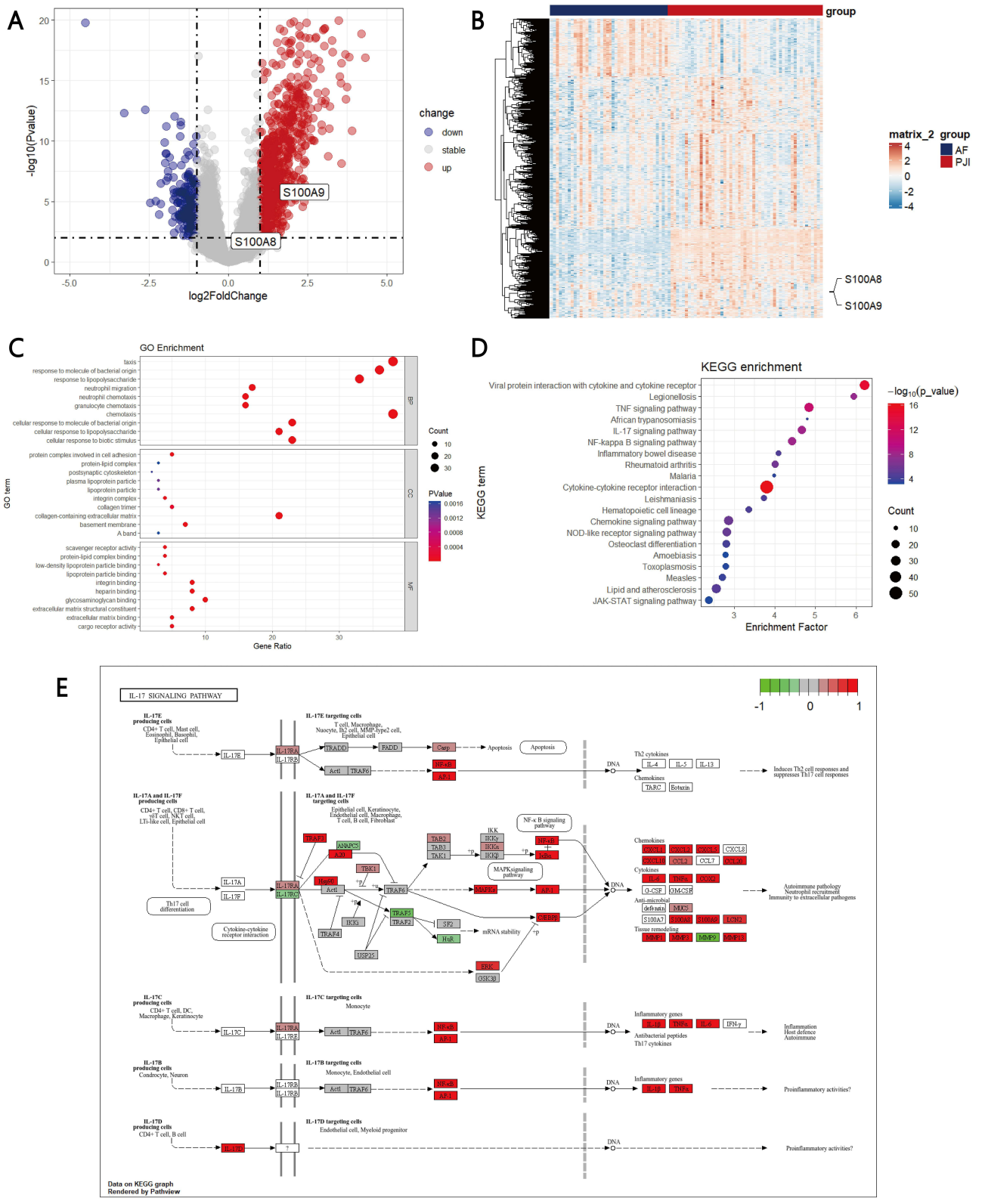

Figure 2 Expression of S100A8 and S100A9 and enrichment analysis of DEGs. (**A**) Volcano map shows S100A8 and S100A9 in up-regulated DEGs of the PJI patients vs AF patients; (**B**) Heatmap shows S100A8 and S100A9 in up-regulated DEGs of the PJI patients vs AF patients; (**C**) GO functional clustering analysis; (**D**) KEGG functional clustering analysis; (**E**) S100A8 and S100A9 were enriched in IL-17 signaling pathway.

https://doi.org/10.2147/IDR.S574816

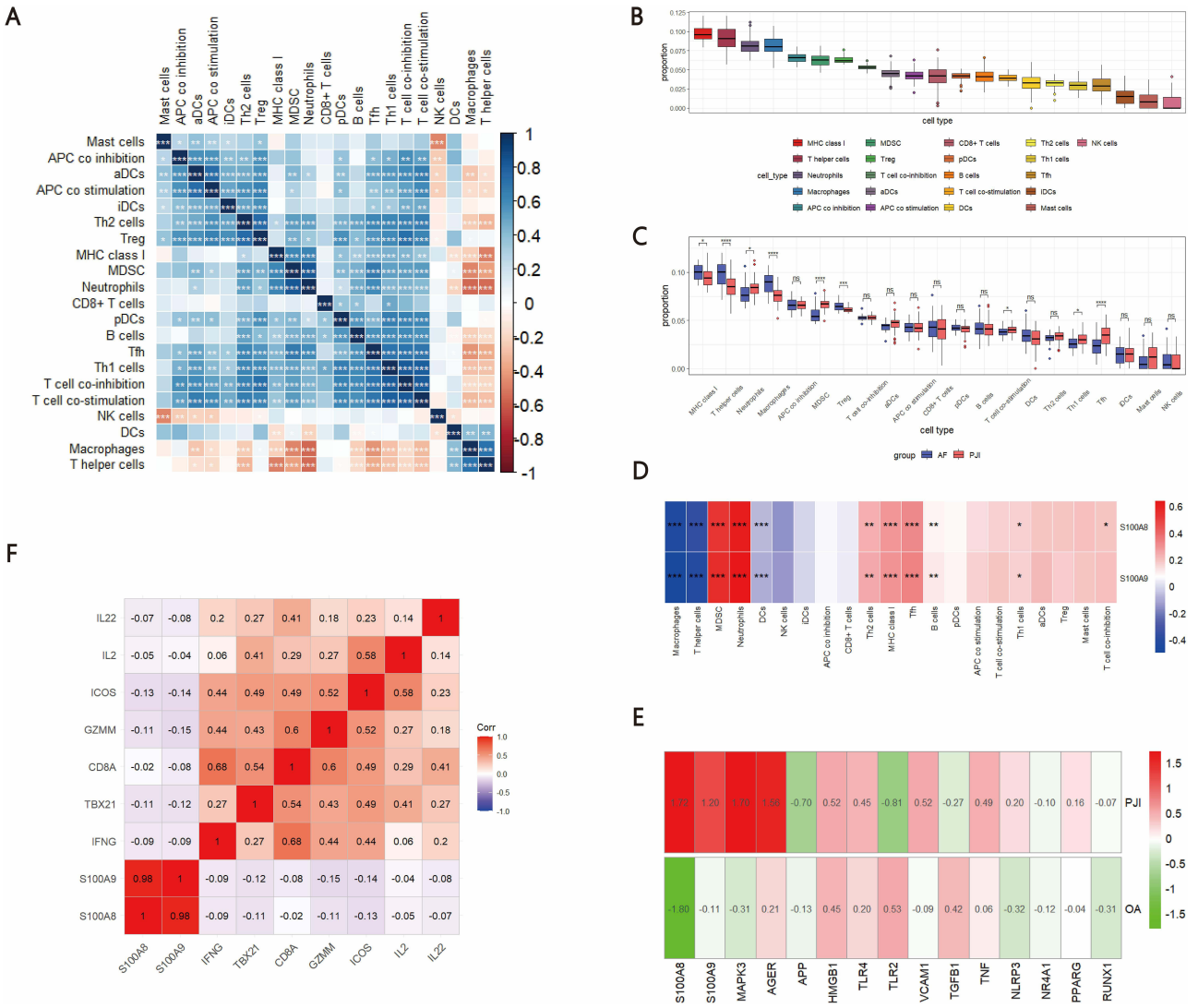

Figure 3 Correlation of S100A8 and S100A9 with immune cell infiltration and immune functional signatures. (**A**) Correlation among immune cell infiltration and immune functional/pathway signatures as quantified by ssGSEA; (**B**) Enrichment scores of 21 immune-related signatures in PJI and AF tissues; (**C**) Differences in immune cell and functional/pathway signature enrichment between PJI and AF patients; (**D**) Correlation of S100A8 and S100A9 expression with the enrichment scores of immune cells and functional/pathway signatures; (**E**) Differential expression of S100A8 and S100A9 in PJI and OA datasets; (**F**) Negative correlation of S100A8 and S100A9 with cytotoxic cytokine expression in $CD8^+$ T cells. *** represents $P < 0.001$, ** represents $P < 0.01$, * represents $P < 0.05$, and ns represents $P > 0.05$.

These findings suggest that elevated S100A8/S100A9 expression is associated with impaired $CD8^+$ T cell cytotoxic function and reduced T cell activation in PJI tissues.

Collectively, these results support an association between elevated S100A8/S100A9 expression and an immunosuppressive microenvironment in PJI tissues, characterized by enrichment of MDSCs and reduced expression of T cell activation–related genes.

Subsequently, we applied the ESTIMATE algorithm to calculate immune scores for the patients. PJI patients exhibited significantly higher ESTIMATE and immune scores compared to AF patients ($P < 0.001$) (Figure S2A–C). We further divided PJI patients into high and low S100A8 expression groups. The high-expression group had higher immune scores (P=0.005) and lower stromal scores (P=0.007) (Figure S2D–F). Similarly, the S100A9 high-expression group also showed higher immune scores (P=0.004) and lower stromal scores (P=0.02) (Figure S2G–I).

https://doi.org/10.2147/IDR.S574816

S100A8 and S100A9 Positively Correlate with MDSC-Related Chemokines

Accumulating evidence indicates that MDSCs are primarily recruited by chemokines such as CXCL1, CXCL5, CXCL6, CXCL8, and CXCL12.[28–30] In line with these observations, our analysis of PJI patient samples revealed a positive correlation between S100A8/S100A9 expression and multiple MDSC-recruiting chemokines (Figure S3A). Specifically, CXCL1, a ligand for CXCR2, was shown to be upregulated in multiple tumor types and recruits MDSCs to the tumor microenvironment via the CXCL1-CXCR2 axis.[31] In our study, both S100A8 and S100A9 were significantly positively correlated with CXCL1 in the local infection microenvironment of PJI (Figure S3B and C). Our data demonstrate that MDSC-recruiting chemokines and S100A8/S100A9 are concurrently upregulated in synovial tissues from PJI patients. However, this observation is purely correlative, and no causal relationship between S100A8/S100A9 and MDSCs infiltration can be inferred from the current data.

Construction of the Single-Cell Transcriptional Landscape in PJI and OA Patients

To determine the cellular sources of calprotectin within the PJI synovial tissue, we integrated two scRNA-seq datasets, including synovial tissue samples from two PJI patients and five OA patients. Among them, 34,818 single cells were derived from OA tissues, and 13,670 cells were from PJI tissues. Unsupervised clustering was performed to visualize specific cell types and identify clusters based on anchored gene expression. A total of 12 clusters and 8 distinct cell types, including adipocytes, B cells, endothelial cells, fibroblasts, macrophages, monocytes, pericyte-like cells, and T cells, were identified (Figure 4A). Representative markers for each cluster are shown in Figure 4B, and the frequency of each cell type across different samples is shown in Figure 4C. In PJI patients, there was a higher percentage of immune cells such as monocytes, whereas in OA patients, a higher percentage of non-immune cells, such as fibroblasts, was observed (Figure 4D). S100A8 and S100A9 are mainly highly expressed in immune cells such as monocytes, macrophages and T cells (Figure 4E). Our findings suggest that S100A8 and S100A9 are predominantly expressed in monocytes, macrophages, and MDSCs, therefore linking synovial tissue calprotectin expression to specific immune cell populations in PJI synovial tissues.

Single-Cell Subset Analysis and Expression of S100A8 and S100A9

We further analyzed synovial macrophages and monocytes in PJI and OA patients following dimensionality reduction and clustering. UMAP dimensionality reduction identified three macrophage clusters: M1, M2, and polymorphonuclear myeloid-derived suppressor cells (PMN-MDSCs) (Figure 5A). Violin plots displayed the expression of S100A8 and S100A9 in the different macrophage subsets where PMN-MDSCs showed the highest levels of S100A8 and S100A9 (Figure 5B). Similarly, monocytes were clustered into five groups: classical monocytes, inflammatory monocytes, intermediate monocytes, monocytic myeloid-derived suppressor cells (M-MDSCs), and non-classical monocytes (Figure 5C). M-MDSCs had the highest expression levels of S100A8 and S100A9 (Figure 5D).

To better understand immune cell infiltration in PJI synovial tissue, we conducted scRNA-seq on synovial tissue samples from 2 PJI patients. Eight cell types were identified, including B cells, fibroblasts, M-MDSCs, macrophages, monocytes, NK cells, PMN-MDSCs, and T cells (Figure 6A). UMAP plots demonstrated the expression patterns of marker genes for each cell type (Figure 6B). PMN-MDSCs were defined based on the co-expression of CEACAM8 and OLR1, consistent with previously reported transcriptomic signatures of neutrophil-like MDSCs (Figure 6B).[32] M-MDSCs were defined by the co-expression of CD14 and ITGAM (CD11b), consistent with previously reported transcriptomic signatures of human monocytic myeloid-derived suppressor cells (Figure 6B).[33] UMAP and violin plots further showed the expression patterns of S100A8 and S100A9 in PJI (Figure 6C and D). The violin plot also highlighted the expression of ITGAM (CD11b), a marker for MDSCs, which was highly expressed in both M-MDSCs and PMN-MDSCs, confirming the presence of MDSCs in the synovial tissue of PJI patients (Figure 6D). In addition, scRNA-seq analyses of PJI patients similarly showed that MDSCs expressed the highest levels of S100A8 and S100A9, with fibroblasts showing the lowest expression (Figure 6D). Our findings suggest that S100A8, S100A9 and MDSCs are involved in the occurrence and development of PJI.

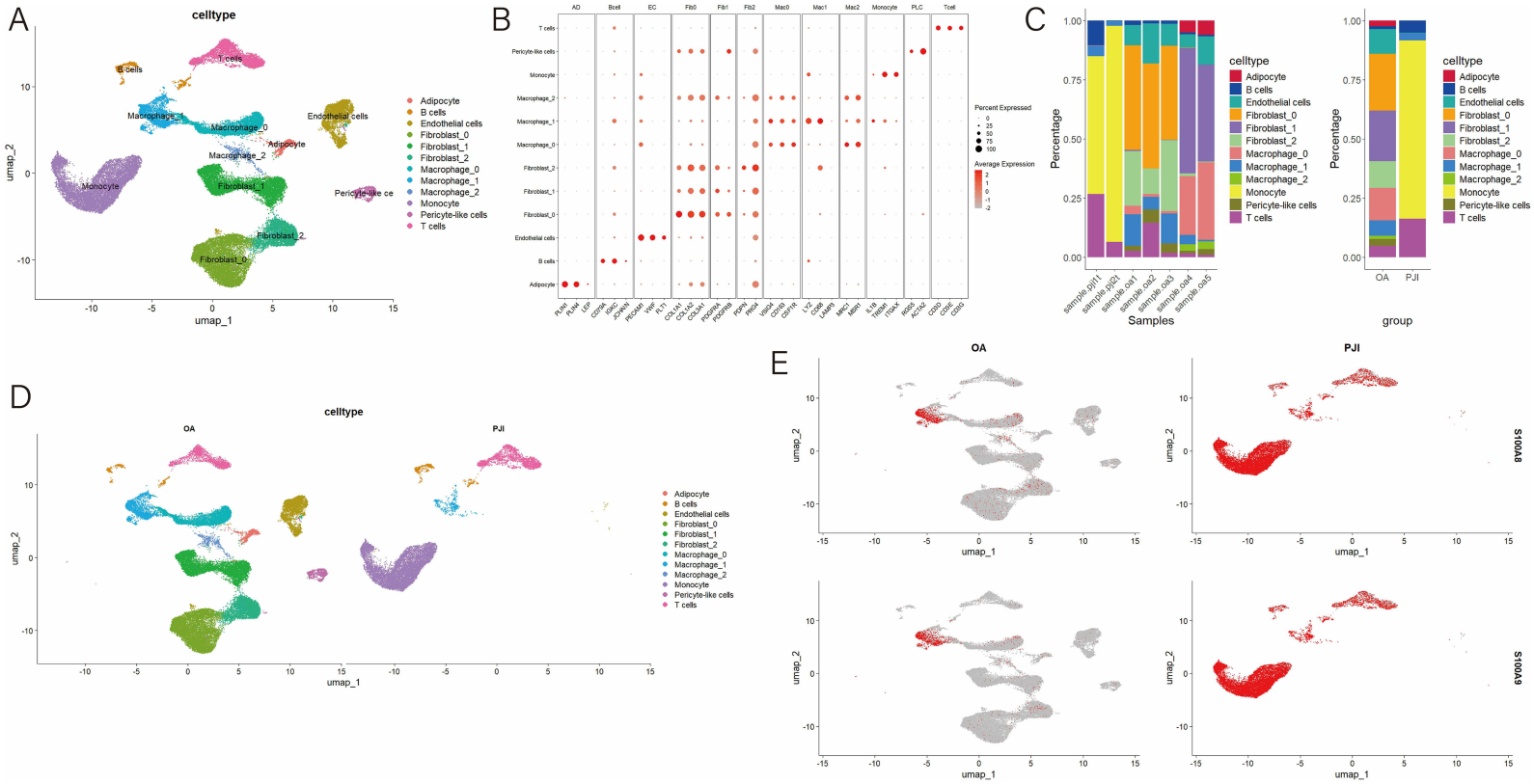

Figure 4 Single cell RNA sequence analysis (**A**) cells were grouped into 12 separate clusters by UMAP; (**B**) Dot plot and heatmap showing the marker genes of each cell type; (**C**) Distribution of different cell types in patients with PJI and OA; (**D**) Frequency of each cell type in different samples; (**E**) Frequency of each cell type in patients with PJI and OA.

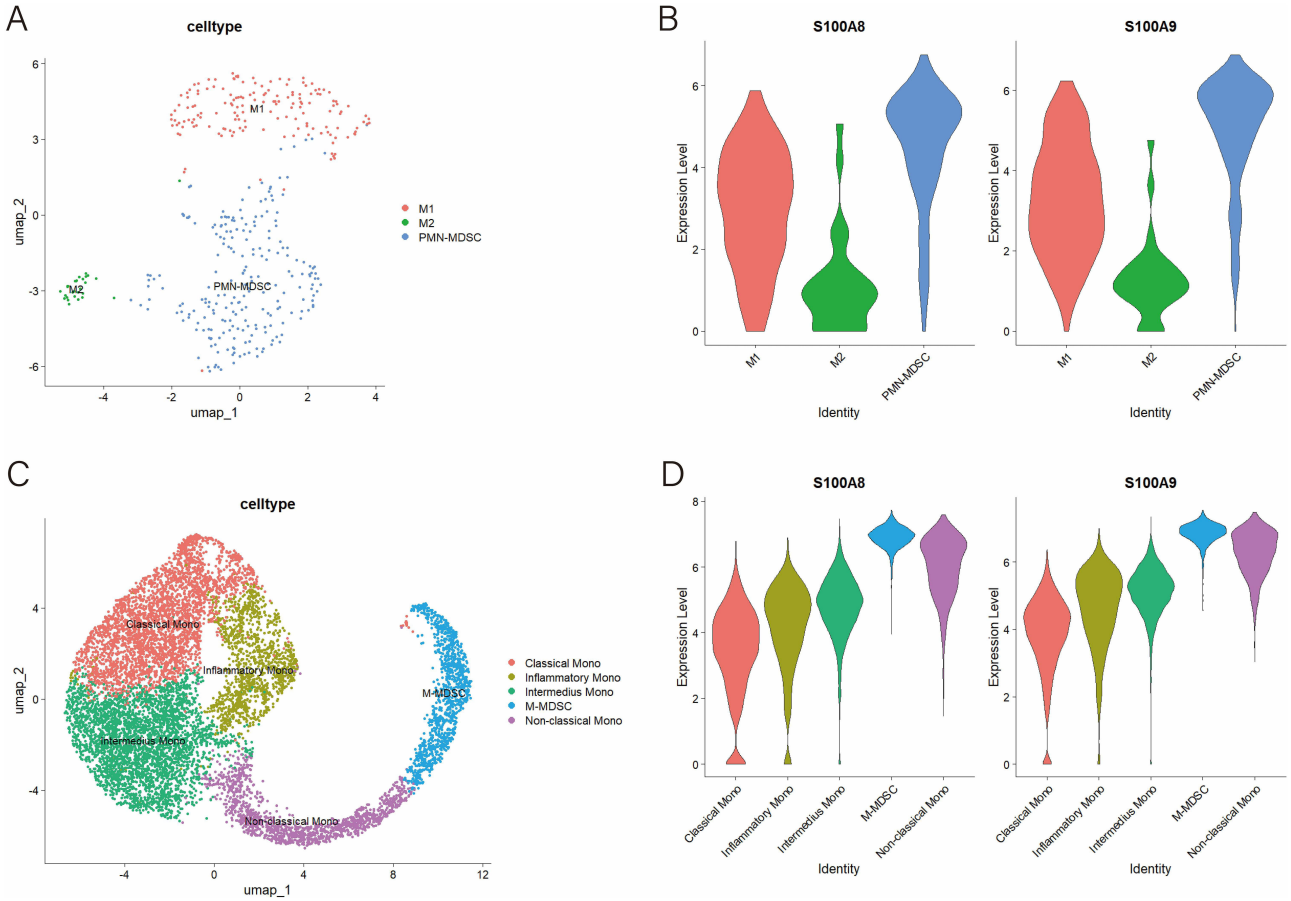

Figure 5 Subset analysis of macrophages and monocytes. (**A**) Macrophages were classified into three subsets; (**B**) Expression levels of S100A8 and S100A9 in three macrophage subsets; (**C**) Monocytes were classified into five subgroups; (**D**) Expression levels of S100A8 and S100A9 in five monocyte subsets.

Cell-Cell Communication in the Immune Microenvironment of PJI

We used the CellChat package to simulate ligand-receptor interactions among different cell types, generating a cell-cell communication network. The analysis revealed extensive interactions between various cell types (Figure 7A and B). Given the established role of TGF-β signaling in infection-associated immunesuppression and MDSCs expansion and functional polarization,[34] we further examined TGF-β-mediated signaling at the pathway level. Consistent with this, pathway analysis identified the TGF-β signaling pathway as a key driver of intercellular communication between PMN-MDSCs and M-MDSCs (Figure 7C and D). Heatmaps and network diagrams highlighted significant interactions between PMN-MDSCs, M-MDSCs, macrophages, and NK cells within the TGF-β signaling pathway (Figure 7C and D). These cell-cell communication patterns in synovial tissue are likely involved in the pathogenesis and development of PJI.

IHC Validation of Calprotectin Expression in PJI Synovial Tissue

To validate the expression and diagnostic value of synovial tissue calprotectin in PJI, we performed a retrospective study of synovial tissues from 100 patients, including 45 patients with PJI, 45 patients with AF, and 10 patients with OA. The baseline information of patients is shown in Table 1. Among the 45 patients diagnosed with PJI, postoperative microbial cultures were positive in 28 cases (62.2%) and negative in 17 cases (37.8%). The most commonly isolated pathogens were Gram-positive bacteria, particularly *Staphylococcus aureus* (including MRSA) and *Staphylococcus epidermidis* (including MRSE). Gram-negative bacteria, such as Pseudomonas aeruginosa, as well as fungal pathogens were identified in a subset of patients. Polymicrobial infections were observed in several cases (Table 2). We performed IHC staining for calprotectin in synovial tissues. Calprotectin was significantly increased in PJI tissues compared with AF and OA tissues (Figure 8A and B). ROC curve analysis was conducted based on the immunostained area of the

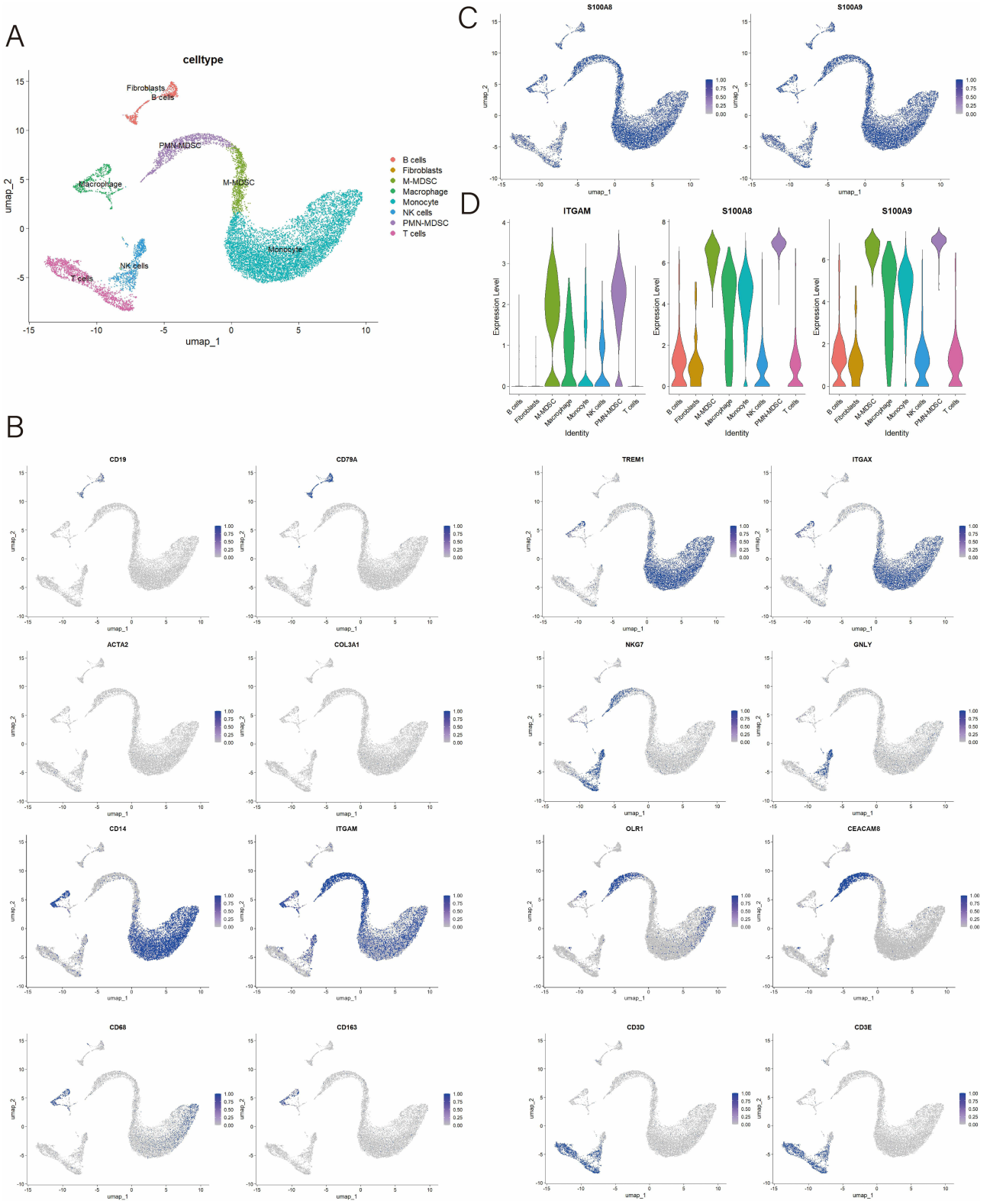

Figure 6 Single-cell RNA sequencing analysis of PJI patients. (**A**) UMAP plots of 8 cell types in PJI patients; (**B**) UMAP plot highlighting the expression patterns of marker genes for the 8 cell types; (**C**) UMAP plot demonstrate the expression of S100A8 and S100A9; (**D**) Violin plots showing the expression of ITGAM, S100A8 and S100A9 in different cell types.

https://doi.org/10.2147/IDR.S574816

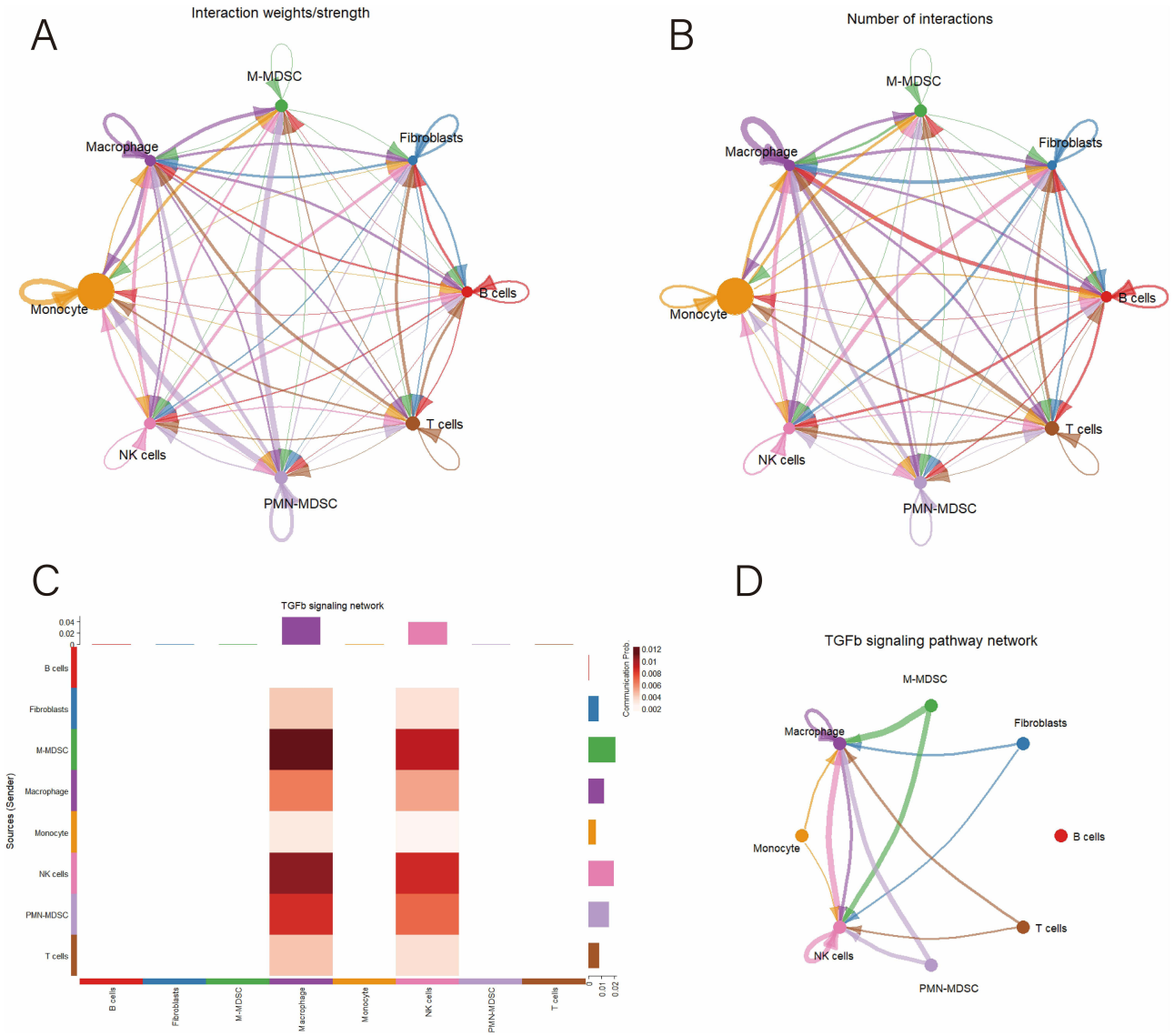

Figure 7 Cell-cell communication analysis. (**A**) Network diagram illustrating the strength of ligand-receptor interactions between different cell types; (**B**) Network diagram illustrating the number of ligand-receptor interactions between different cell types; (**C**) Heatmap illustrating the interaction patterns of ligand-receptor interactions in the TGFb signaling pathway across different cell types; (**D**) Intercellular communication network diagram within the TGFb signaling pathway; (**E**) Upregulated receptor-ligand interaction networks between PMN-MDSCs and other cell types; (**F**) Upregulated receptor-ligand interaction networks between M-MDSCs and other cell types.

S100A8/A9 complex and bulk RNA sequencing data (Figure 8C). Bulk RNA sequencing yielded AUC values of 0.71 for S100A8 and 0.73 for S100A9, whereas the IHC-based analysis demonstrated a higher diagnostic performance with an AUC of 0.85. Using Youden's index criteria (optimal cut-off value: 22.60% positive area), calprotectin staining demonstrated a sensitivity of 77.78% (95% CI: 63.73–87.46%) and a specificity of 86.67% (95% CI: 73.82–93.74%).

Table 1 Baseline Information of PJI, AF, and OA Patients

	PJI	AF	OA	P value
Sex (F/M)	26/19	23/22	7/3	>0.05
Age	73.87±8.00	72.04±7.76	68.22±12.02	>0.05
Joint (Hip/Knee)	30/15	28/17	6/4	>0.05
Time of implantation (months)	43.04±49.56	97.60±45.38	Not Applicable	<0.001
CRP (mg/L)	53.81±34.14	6.31±13.64	3.29±1.49	<0.001
ESR (mm/h)	97.42±13.24	27.98±13.77	7.70±2.06	<0.001

https://doi.org/10.2147/IDR.S574816

Table 2 Microbiological Characteristics of Patients with PJI

Pathogen Category	Isolated Pathogens	No. of Cases (n = 45)
Culture-negative	No pathogen isolated	17
Gram-positive bacteria	*Staphylococcus aureus* (including MRSA)	12
	Staphylococcus epidermidis (including MRSE)	6
	Other Gram-positive bacteria[†]	3
Gram-negative bacteria	Pseudomonas aeruginosa	4
	Escherichia coli	1
	Salmonella typhimurium	1
Fungal infection	Fungal pathogens	3
Polymicrobial infection	Mixed bacterial/fungal species	2

Notes: [†]Other Gram-positive bacteria include *Corynebacterium striatum, Staphylococcus kloosii, Propionibacterium acnes*, and *Streptococcus* species.

Further subgroup analyses were conducted to compare calprotectin IHC staining results between AF cases and PJI patients stratified by postoperative culture status. In culture-positive PJI cases, the staining demonstrated an AUC of 0.85 with an optimal cut-off value of 22.60% positive area, showing 78.57% sensitivity (95% CI: 60.46–89.79%) and 86.67% specificity (95% CI: 73.82–93.74%). For culture-negative PJI cases, the diagnostic performance remained robust with an AUC of 0.84 at a cut-off of 23.29% positive area, achieving 76.47% sensitivity (95% CI: 52.74–90.44%) and 86.67% specificity (95% CI: 73.82–93.74%) (Figure 8D).

Furthermore, we conducted subgroup analyses based on the timing of PJI onset. Patients who developed PJI within 3 months after TJA were classified as early PJI cases (n=17), while those who developed PJI beyond 3 months post-operatively were categorized as late PJI cases (n=28). For early PJI, calprotectin IHC staining demonstrated an AUC of 0.83, with an optimal cut-off value of 23.81% positive staining area. At this threshold, the sensitivity was 70.59% (95% CI: 46.87–86.72%), and the specificity was 86.67% (95% CI: 73.82–93.74%). For late PJI, the optimal cut-off value was 22.60% positive staining areas, and calprotectin IHC staining achieved an AUC of 0.86, with a sensitivity of 82.14% (95% CI: 64.41–92.12%) and a specificity of 86.67% (95% CI: 73.82–93.74%) (Figure 8E). Taken together, our findings

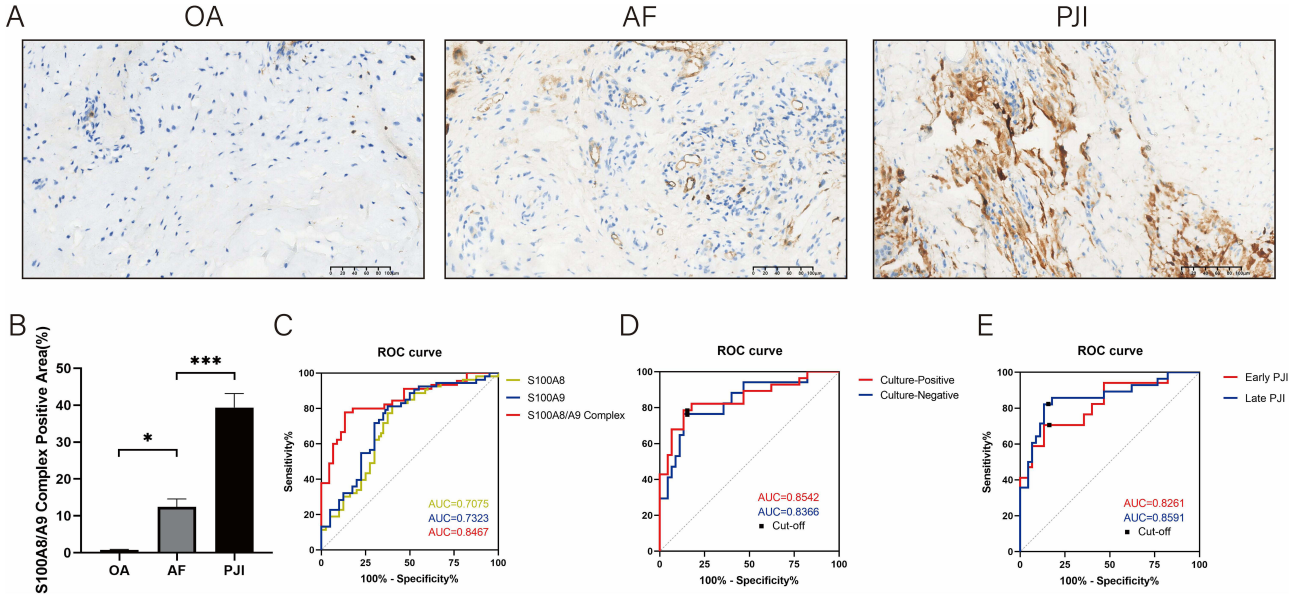

Figure 8 Analysis of immunostaining results and diagnostic value of the S100A8/A9 complex. (**A**) Representative images of immunohistochemical staining for S100A8/A9 complex in patients with OA, AF, PJI; (**B**) Quantitative analysis of immunohistochemical staining for S100A8/A9 complex in patients with OA, AF, PJI; (**C**) ROC curve analysis of S100A8, S100A9 and S100A8/A9 complex by integrated bulk RNA sequencing and immunohistochemical staining; (**D**) ROC curve analysis of culture-positive and culture-negative PJI patients. (**E**) ROC curve analysis of early and late PJI patients. *** represents P < 0.001, * represents P < 0.05.

https://doi.org/10.2147/IDR.S574816

support synovial tissue calprotectin (S100A8/A9) as a reliable diagnostic biomarker for PJI, with preserved diagnostic performance in culture-negative and early-onset infections, underscoring its value as a complementary tool to conventional microbiological diagnostics.

Discussion

In this study, we integrated bulk RNA-seq and scRNA-seq data to demonstrate that calprotectin (S100A8/A9) serves as a diagnostic biomarker for PJI in synovial tissue. Although calprotectin (S100A8/A9) has been previously reported as a diagnostic biomarker for PJI, most prior studies focused on its measurement in synovial fluid and did not address its cellular origin or immunological context within infected tissues.[14,16,35] In this study, by integrating bulk RNA sequencing, single-cell transcriptomics, cell-cell communication analysis, and tissue-level validation, we demonstrate that calprotectin expression within synovial tissue is predominantly driven by MDSCs and is closely linked to a TGF-β immunosuppressive microenvironment involving macrophages and NK cells. These findings extend the role of synovial tissue calprotectin from a nonspecific inflammatory marker to an MDSC-dominated immunosuppressive dysregulation in PJI. Importantly, our IHC-based validation further supports synovial tissue calprotectin as a practical diagnostic marker for culture-negative and early-stage PJI, complementing existing synovial fluid-based diagnostics. Preoperative aspiration of cancer sites and IHC staining for precise molecular diagnosis of various cancers are well-established techniques.[36,37] Given the high expression of calprotectin in synovial tissue in PJI cases, we recommend preoperative joint aspiration with calprotectin IHC staining or synovial fluid protein analysis for patients with challenging PJI diagnoses, as these approaches may significantly improve diagnostic accuracy. Additionally, adjuvant pharmacological therapy based on calprotectin expression levels before revision surgery could optimize treatment outcomes and minimize PJI recurrence.

PJI is the third most common complication following TJA, accounting for 15.3% of cases after aseptic loosening (36.5%) and prosthesis dislocation (17.7%).[38] Despite its prevalence, little is known about the immune response in the tissues surrounding infected implants. The primary pathogens responsible for PJI are *Staphylococcus aureus* and coagulase-negative staphylococci, which account for 50–60% of cases.[39] By recruiting MDSCs to infection sites, *S. aureus* induces T-cell suppression, thereby promoting bacterial persistence.[40,41] In our study, we found that MDSCs aggregated in PJI tissues, which could explain the persistence of the infection.

Given the heterogeneity of causative pathogens in PJI, we further explored whether S100A8/A9 expression differed according to infective species. Subgroup analyses demonstrated that S100A8/A9 expression was elevated across all pathogen-defined PJI subgroups compared with AF group, with the highest levels observed in *S. aureus* PJI, while *S. epidermidis* PJI showed a more modest increase. This gradient of expression may reflect differences in pathogen virulence and the magnitude of the host inflammatory response, as *S. aureus* infections are typically associated with stronger neutrophil-dominated inflammatory responses, whereas *S. epidermidis* PJI often presents as a low-grade, biofilm-associated inflammatory process.[17,42] Importantly, when PJI cases were analyzed as a pooled group regardless of pathogen type, S100A8/A9 expression remained significantly elevated compared with AF, supporting its consistent upregulation in PJI synovial tissues independent of the specific infective pathogen.

S100A8 and S100A9 are released from neutrophils and monocytes/macrophages during PJI flare-ups, following Toll-like receptor 4 activation. These proteins act as damage-associated molecular patterns (DAMPs), driving the upregulation of pro-inflammatory cytokines and increasing local inflammation.[12,43] Our bulk RNA sequencing analysis revealed correlations between S100A8/S100A9 and multiple chemokines. Both bulk RNA sequencing and scRNA-seq showed strong correlations between S100A8/S100A9 expression and MDSCs abundance. Importantly, this correlation likely reflects, at least in part, the fact that MDSCs themselves are a major source of S100A8/A9, and that in the PJI immune microenvironment, chemokine-mediated recruitment may result in an expanded MDSC population with increased S100A8/A9 expression, rather than solely indicating S100A8/A9-mediated recruitment of MDSCs.[44,45] While consistent with an expanded MDSCs population in PJI, these data are observational and do not establish causality. Previous studies support our findings, showing that MDSCs express high levels of S100A8 and S100A9,[46] and these cells can suppress T-cell responses in inflammatory diseases.[19] Additionally, our study demonstrated a negative correlation between S100A8/S100A9 expression and CD8+ T-cell effector molecules. Consistent with this observation, the negative correlations between S100A8/S100A9 and key $CD8^+$ T cell effector genes (including IFNG, GZMM, CD8A, and TBX21) further support a link between calprotectin-associated inflammation and T cell

dysfunction in PJI. Given the known role of S100A8/S100A9 in promoting MDSCs expansion and immunosuppressive signaling, these findings suggest that elevated calprotectin may contribute to impaired cytotoxic T cell responses within the infected joint microenvironment. It should be noted that neutrophils are well-recognized as major sources of calprotectin. Although neutrophils were prominently represented in the bulk RNA-seq-based immune infiltration analysis, they were not distinctly identified in the scRNA-seq datasets. This discrepancy is likely due to technical limitations of scRNA-seq, as neutrophils are particularly susceptible to degradation during tissue dissociation and often exhibit low RNA content.[47,48] Consequently, the single-cell analyses in this study primarily captured monocyte-, macrophage-, and MDSC-related populations, while neutrophil-associated calprotectin expression is more comprehensively reflected in the bulk transcriptomic data.

Studies in mice have shown that MDSC-mediated NK cell inhibition is primarily driven by TGF-β.[49] Membrane-bound TGF-β suppresses NKG2D expression and IFN-γ production in NK cells, thereby compromising their cytotoxic activity. This mechanism has been validated in murine liver cancer models.[50] MDSCs also promote M2 macrophage polarization and inhibit antigen presentation by dendritic cells through TGF-β secretion.[51,52] Consistent with these findings, our analysis showed that MDSCs interact with NK cells and macrophages in PJI tissues via the TGF-β signaling pathway.

Despite current preventive and therapeutic strategies for PJI, including antibiotic-loaded bone cement, povidone-iodine irrigation during total joint arthroplasty, and intraoperative vancomycin powder, reinfection rates remain as high as 14%.[2,53,54] This ongoing challenge suggests that factors beyond antimicrobial resistance, such as the local immune microenvironment, may influence bacterial persistence and treatment outcomes. Based on our analysis of calprotectin expression and MDSC enrichment, an immunosuppressive microenvironment in PJI may represent an additional factor contributing to bacterial persistence and variable treatment outcomes, beyond antimicrobial resistance. Emerging evidence indicates that immunomodulatory approaches could serve as adjunctive strategies in PJI management. For example, Yamada et al[55] demonstrated that enhancement of pro-inflammatory immune responses improved antibiotic efficacy in experimental PJI models. In addition, our recent work identified MDSC-mediated recruitment of regulatory T cells via the CXCL16–CXCR6 axis as a potential contributor to local immunosuppression, and modulation of this pathway was associated with improved disease features in preclinical settings.[56] While these observations are preliminary, they suggest that future studies may explore immune-targeted interventions, including selective modulation of suppressive immune pathways or cautious application of immune checkpoint blockade, in combination with antibiotic therapy. Such approaches warrant careful evaluation to balance antimicrobial efficacy with safety considerations in PJI management.[57]

Diagnosing PJI remains a major challenge for orthopedic surgeons, with a lack of accurate and cost-effective methods. Although the MSIS criteria assist in diagnosing PJI, bacterial cultures are often negative. Culture-negative PJI prevalence ranges from 5% to 42%.[58] The causes of culture-negative PJI include low-toxicity microbial infections, early antibiotic administration, and the inability to culture bacteria in enriched media.[59] To improve diagnostic accuracy, new laboratory methods such as molecular diagnostics, antigen and antibody assays, and biomarker detection have been introduced in recent years.[60] Our tissue-level analysis supports calprotectin as a synovial tissue diagnostic biomarker for PJI, with diagnostic value observed not only in culture-negative PJI but also in early-stage PJI. In our retrospective analysis of 45 PJI cases, we identified 17 culture-negative instances (37.8%). Notably, calprotectin maintained high diagnostic accuracy across both culture-positive (AUC = 0.85) and culture-negative subgroups (AUC=0.84). Moreover, our analysis demonstrated that calprotectin maintained diagnostic reliability regardless of infection timing, with early PJI cases showing an AUC of 0.83 while late PJI cases achieved an AUC of 0.86.

Accurate diagnosis of early-stage and culture-negative PJI remains clinically challenging, as conventional microbiological methods and standard biomarkers often show limited sensitivity in these settings.[61,62] From a clinical perspective, synovial tissue calprotectin IHC may be particularly valuable in cases of suspected PJI with inconclusive microbiological results, such as culture-negative infections or in patients who received antibiotics prior to sampling. The assessment of calprotectin based on synovial tissue could serve as an adjunct to current diagnostic criteria, providing localized immune information that complements synovial fluid and systemic biomarkers, and may improve diagnostic confidence in early and culture-negative PJI.

Although a wide range of cytokines and biomarkers have been studied from a systemic perspective,[63,64] their clinical utility remains controversial.[65,66] S100A8 and S100A9, subunits of calprotectin, have been investigated for their diagnostic value in synovial fluid for PJI.[11,13] However, it is well known that inflammatory diseases can trigger pathogen responses,

leading to elevated synovial fluid calprotectin and false-positive results.[16] Furthermore, the biological significance of elevated S100A8/A9 expression in PJI remains underexplored, which limits the credibility of S100A8/A9 as a biomarker. Examining cytokine responses at the tissue level may provide a more accurate picture of the local immune environment, offering clinicians better insights into managing postoperative complications through surgical debridement. Previous studies have highlighted the importance of analyzing local cytokine concentrations in PJI patients.[67] Our study compared S100A8/A9 expression in synovium from OA, AF, and PJI patients, finding it absent in OA patients, present to a small extent in AF patients, and significantly elevated in PJI patients. These findings support our bulk RNA sequencing and scRNA-seq analyses and suggest that S100A8/A9 is a promising tissue biomarker for PJI diagnosis.

There are several limitations to this study. First, the number of publicly available PJI datasets is limited, and the sample sizes within each dataset are relatively small, which may not represent the entire PJI patient population. Second, the study was conducted at a single center with a small sample size. Third, the comparatively smaller OA cases (n=10) relative to the PJI and AF groups may limit the generalizability of our findings regarding calprotectin's diagnostic specificity across distinct joint pathologies. Future studies with larger cohorts are needed to validate our findings.

Conclusion

In conclusion, our study shows that S100A8/S100A9 expression in PJI synovial tissue is predominantly associated with MDSCs. Moreover, tissue-level calprotectin demonstrates diagnostic utility for PJI, including early-stage and culture-negative cases. This diagnostic relevance is consistent with the association of calprotectin with an MDSC-enriched immune microenvironment in PJI synovial tissue.

Abbreviations

PJI, Periprosthetic joint infection; AF, Aseptic failure; RNA-seq, Bulk RNA sequencing; scRNA-seq, Single-cell RNA sequencing; MDSCs, Myeloid-derived suppressor cells; ROC, Receiver operating characteristic; TJA, Total joint arthroplasty; MSIS, Musculoskeletal infection society; CRP, C-reactive protein; IHC, Immunohistochemical staining; OA, Osteoarthritis; DEGs, Differentially expressed genes; GO, Gene ontology; BP, Biological processes; MF, Molecular functions; CC, Cellular components; KEGG, Kyoto encyclopedia of genes and genomes; PCA, Principal component analysis; ssGSEA, Single-sample gene set enrichment analysis; M-MDSCs, Monocytic myeloid-derived suppressor cells; PMN-MDSCs, Polymorphonuclear myeloid-derived suppressor cells.

Funding

This study was funded by grants from the Postdoctoral Fellowship Program of CPSF (GZC20233275), Postdoctoral Science Foundation (2024M753776) and the National Natural Science Foundation of China (82372424).

Disclosure

The authors report no conflicts of interest in this work.

References

1. Zeng ZJ, Yao FM, He W, et al. Incidence of periprosthetic joint infection after primary total Hip arthroplasty is underestimated: a synthesis of meta-analysis and bibliometric analysis. *J Orthop Surg Res*. 2023;18(1):610. doi:10.1186/s13018-023-04060-5
2. Izakovicova P, Borens O, Trampuz A. Periprosthetic joint infection: current concepts and outlook. *EFORT Open Rev*. 2019;4(7):482–494. doi:10.1302/2058-5241.4.180092
3. Masters TL, Bhagwate AV, Dehankar MK, et al. Human transcriptomic response to periprosthetic joint infection. *Gene*. 2022;825:146400. doi:10.1016/j.gene.2022.146400
4. Li C, Ojeda-Thies C, Xu C, et al. Meta-analysis in periprosthetic joint infection: a global bibliometric analysis. *J Orthop Surg Res*. 2020;15(1):251. doi:10.1186/s13018-020-01757-9
5. Parvizi J, Zmistowski B, Berbari EF, et al. New definition for periprosthetic joint infection: from the workgroup of the musculoskeletal infection society. *Clin Orthop Relat Res*. 2011;469(11):2992–2994. doi:10.1007/s11999-011-2102-9
6. Parvizi J, Tan TL, Goswami K, et al. The 2018 definition of periprosthetic hip and knee infection: an evidence-based and validated criteria. *J Arthroplasty*. 2018;33(5):1309–1314e2. doi:10.1016/j.arth.2018.02.078
7. Fu Y, Li Q, Zhao H, et al. Construction and evaluation of a combined diagnostic model for chronic periprosthetic joint infection based on serological tests. *J Orthop Surg Res*. 2024;19(1):667. doi:10.1186/s13018-024-05146-4

8. Lee JS, Lee NR, Kashif A, et al. S100A8 and S100A9 promote apoptosis of chronic eosinophilic leukemia cells. *Front Immunol*. 2020;11:1258. doi:10.3389/fimmu.2020.01258
9. Leukert N, Vogl T, Strupat K, et al. Calcium-dependent tetramer formation of S100A8 and S100A9 is essential for biological activity. *J Mol Biol*. 2006;359(4):961–972. doi:10.1016/j.jmb.2006.04.009
10. Sohnle PG, Hunter MJ, Hahn B, et al. Zinc-reversible antimicrobial activity of recombinant calprotectin (migration inhibitory factor-related proteins 8 and 14). *J Infect Dis*. 2000;182(4):1272–1275. doi:10.1086/315810
11. Warren JA, Klika AK, Bowers K, et al. Calprotectin lateral flow test: consistent across criteria for ruling out periprosthetic joint infection. *J Arthroplasty*. 2022;37(6):1153–1158. doi:10.1016/j.arth.2022.01.082
12. Grassi M, Salari P, Farinelli L, et al. Synovial biomarkers to detect chronic periprosthetic joint infection: a pilot study to compare calprotectin rapid test, calprotectin elisa immunoassay and leukocyte esterase test. *J Arthroplasty*. 2022;37(4):781–786. doi:10.1016/j.arth.2021.12.040
13. Sowislok A, Busch A, Kaschani F, et al. Differences in the synovial fluid proteome of septic and aseptic implant failure. *Antibiotics*. 2024;13(4). doi:10.3390/antibiotics13040346
14. Wouthuyzen-Bakker M, Ploegmakers JJW, Kampinga GA, et al. Synovial calprotectin: a potential biomarker to exclude a prosthetic joint infection. *Bone Joint J*. 2017;99-B(5):660–665. doi:10.1302/0301-620X.99B5.BJJ-2016-0913.R2
15. Baishya J, Everett JA, Chazin WJ, et al. The innate immune protein calprotectin interacts with and encases biofilm communities of Pseudomonas aeruginosa and *Staphylococcus aureu*s. *Front Cell Infect Microbiol*. 2022;12:898796. doi:10.3389/fcimb.2022.898796
16. Zhang Z, Cai Y, Bai G, et al. The value of calprotectin in synovial fluid for the diagnosis of chronic prosthetic joint infection. *Bone Joint Res*. 2020;9(8):450–457. doi:10.1302/2046-3758.98.BJR-2019-0329.R2
17. Lazic I, Prodinger P, Stephan M, et al. Synovial calprotectin is a reliable biomarker for periprosthetic joint infections in acute-phase inflammation - a prospective cohort study. *Int Orthop*. 2022;46(7):1473–1479. doi:10.1007/s00264-022-05421-1
18. Alkadhem MF, Ettema H, Wagenmakers-Huizenga LMF, et al. Synovial calprotectin is superior to synovial leukocyte count in excluding chronic periprosthetic joint infections, a retrospective cohort study. *J Arthroplasty*. 2024;39(8):1926–1931e1. doi:10.1016/j.arth.2024.02.064
19. Gabrilovich DI, Nagaraj S. Myeloid-derived suppressor cells as regulators of the immune system. *Nat Rev Immunol*. 2009;9(3):162–174. doi:10.1038/nri2506
20. Sinha P, Okoro C, Foell D, et al. Proinflammatory S100 proteins regulate the accumulation of myeloid-derived suppressor cells. *J Immunol*. 2008;181(7):4666–4675. doi:10.4049/jimmunol.181.7.4666
21. Tarabichi M, Shohat N, Goswami K, et al. Diagnosis of periprosthetic joint infection: the potential of next-generation sequencing. *J Bone Joint Surg Am*. 2018;100(2):147–154. doi:10.2106/JBJS.17.00434
22. Roh J, Jeon J, Jo S, et al. Gene profiling analyses of synovium tissues in korean osteoarthritis patients. *In Vivo*. 2025;39(6):3128–3142. doi:10.21873/invivo.14114
23. Horn CM, Arumugam P, Van Roy Z, et al. Granulocytic myeloid-derived suppressor cell activity during biofilm infection is regulated by a glycolysis/HIF1a axis. *J Clin Invest*. 2024;134(8). doi:10.1172/JCI174051
24. Tang S, Yao L, Ruan J, et al. Single-cell atlas of human infrapatellar fat pad and synovium implicates APOE signaling in osteoarthritis pathology. *Sci Transl Med*. 2024;16(731):eadf4590. doi:10.1126/scitranslmed.adf4590
25. Bindea G, Mlecnik B, Tosolini M, et al. Spatiotemporal dynamics of intratumoral immune cells reveal the immune landscape in human cancer. *Immunity*. 2013;39(4):782–795. doi:10.1016/j.immuni.2013.10.003
26. Konsti J, Lundin M, Linder N, et al. Effect of image compression and scaling on automated scoring of immunohistochemical stainings and segmentation of tumor epithelium. *Diagn Pathol*. 2012;7(29). doi:10.1186/1746-1596-7-29
27. Bai S, Wang W, Ye L, et al. IL-17 stimulates neutrophils to release S100A8/A9 to promote lung epithelial cell apoptosis in Mycoplasma pneumoniae-induced pneumonia in children. *Biomed Pharmacother*. 2021;143:112184. doi:10.1016/j.biopha.2021.112184
28. Kumar V, Patel S, Tcyganov E, et al. The nature of myeloid-derived suppressor cells in the tumor microenvironment. *Trends Immunol*. 2016;37(3):208–220. doi:10.1016/j.it.2016.01.004
29. Li BH, Garstka MA, Li ZF. Chemokines and their receptors promoting the recruitment of myeloid-derived suppressor cells into the tumor. *Mol Immunol*. 2020;117:201–215. doi:10.1016/j.molimm.2019.11.014
30. Ozga AJ, Chow MT, Luster AD. Chemokines and the immune response to cancer. *Immunity*. 2021;54(5):859–874. doi:10.1016/j.immuni.2021.01.012
31. Cheng Y, Ma XL, Wei YQ, et al. Potential roles and targeted therapy of the CXCLs/CXCR2 axis in cancer and inflammatory diseases. *Biochim Biophys Acta Rev Cancer*. 2019;1871(2):289–312. doi:10.1016/j.bbcan.2019.01.005
32. Condamine T, Dominguez GA, Youn JI, et al. Lectin-type oxidized LDL receptor-1 distinguishes population of human polymorphonuclear myeloid-derived suppressor cells in cancer patients. *Sci Immunol*. 2016;1(2). doi:10.1126/sciimmunol.aaf8943
33. Bronte V, Brandau S, Chen SH, et al. Recommendations for myeloid-derived suppressor cell nomenclature and characterization standards. *Nat Commun*. 2016;7:12150. doi:10.1038/ncomms12150
34. Hao Z, Li R, Wang Y, et al. Landscape of myeloid-derived suppressor cell in tumor immunotherapy. *Biomark Res*. 2021;9(1):77. doi:10.1186/s40364-021-00333-5
35. Hantouly AT, Salameh M, Toubasi AA, et al. Synovial fluid calprotectin in diagnosing periprosthetic joint infection: a meta-analysis. *Int Orthop*. 2022;46(5):971–981. doi:10.1007/s00264-022-05357-6
36. Sipos JA, Ringel MD. Molecular testing in thyroid cancer diagnosis and management. *Best Pract Res Clin Endocrinol Metab*. 2023;37(1):101680. doi:10.1016/j.beem.2022.101680
37. Raychaudhuri R, Lin DW, Montgomery RB. Prostate cancer: a review. *JAMA*. 2025;333(16):1433–1446. doi:10.1001/jama.2025.0228
38. Otto-Lambertz C, Yagdiran A, Wallscheid F, et al. Periprosthetic infection in joint replacement. *Dtsch Arztebl Int*. 2017;114(20):347–353. doi:10.3238/arztebl.2017.0347
39. Tande AJ, Patel R. Prosthetic joint infection. *Clin Microbiol Rev*. 2014;27(2):302–345. doi:10.1128/CMR.00111-13
40. Heim CE, Vidlak D, Scherr TD, et al. IL-12 promotes myeloid-derived suppressor cell recruitment and bacterial persistence during *Staphylococcus aureu*s orthopedic implant infection. *J Immunol*. 2015;194(8):3861–3872. doi:10.4049/jimmunol.1402689
41. Peng KT, Hsieh CC, Huang TY, et al. *Staphylococcus aureus* biofilm elicits the expansion, activation and polarization of myeloid-derived suppressor cells in vivo and in vitro. *PLoS One*. 2017;12(8):e0183271. doi:10.1371/journal.pone.0183271

42. Schindler M, Walter N, Maderbacher G, et al. Novel diagnostic markers for periprosthetic joint infection: a systematic review. *Front Cell Infect Microbiol*. 2023;13:1210345. doi:10.3389/fcimb.2023.1210345
43. Vogl T, Gharibyan AL, Morozova-Roche LA. Pro-inflammatory S100A8 and S100A9 proteins: self-assembly into multifunctional native and amyloid complexes. *Int J Mol Sci*. 2012;13(3):2893–2917. doi:10.3390/ijms13032893
44. von Wulffen M, Luehrmann V, Robeck S, et al. S100A8/A9-alarmin promotes local myeloid-derived suppressor cell activation restricting severe autoimmune arthritis. *Cell Rep*. 2023;42(8):113006. doi:10.1016/j.celrep.2023.113006
45. Yang Y, Zhang X, Jing L, et al. MDSC-derived S100A8/9 contributes to lupus pathogenesis by promoting TLR7-mediated activation of macrophages and dendritic cells. *Cell Mol Life Sci*. 2024;81(1):110. doi:10.1007/s00018-024-05155-w
46. Yang J, Anholts J, Kolbe U, et al. Calcium-binding proteins S100A8 and S100A9: investigation of their immune regulatory effect in myeloid cells. *Int J Mol Sci*. 2018;19(7). doi:10.3390/ijms19071833
47. Salcher S, Sturm G, Horvath L, et al. High-resolution single-cell atlas reveals diversity and plasticity of tissue-resident neutrophils in non-small cell lung cancer. *Cancer Cell*. 2022;40(12):1503–1520e8. doi:10.1016/j.ccell.2022.10.008
48. Wigerblad G, Cao Q, Brooks S, et al. Single-cell analysis reveals the range of transcriptional states of circulating human neutrophils. *J Immunol*. 2022;209(4):772–782. doi:10.4049/jimmunol.2200154
49. Li Z, Pang Y, Gara SK, et al. Gr-1+CD11b+ cells are responsible for tumor promoting effect of TGF-beta in breast cancer progression. *Int J Cancer*. 2012;131(11):2584–2595. doi:10.1002/ijc.27572
50. Li H, Han Y, Guo Q, et al. Cancer-expanded myeloid-derived suppressor cells induce anergy of NK cells through membrane-bound TGF-beta 1. *J Immunol*. 2009;182(1):240–249. doi:10.4049/jimmunol.182.1.240
51. Ugolini A, Tyurin VA, Tyurina YY, et al. Polymorphonuclear myeloid-derived suppressor cells limit antigen cross-presentation by dendritic cells in cancer. *JCI Insight*. 2020;5(15). doi:10.1172/jci.insight.138581
52. Joshi S, Sharabi A. Targeting myeloid-derived suppressor cells to enhance natural killer cell-based immunotherapy. *Pharmacol Ther*. 2022;235:108114. doi:10.1016/j.pharmthera.2022.108114
53. Wu Y, Xiang X, Ma Y. The effect of different preventive strategies during total joint arthroplasty on periprosthetic joint infection: a network meta-analysis. *J Orthop Surg Res*. 2024;19(1):360. doi:10.1186/s13018-024-04738-4
54. Liao S, Yang Z, Li X, et al. Effects of different doses of vancomycin powder in total knee and Hip arthroplasty on the periprosthetic joint infection rate: a systematic review and meta-analysis. *J Orthop Surg Res*. 2022;17(1):546. doi:10.1186/s13018-022-03445-2
55. Yamada KJ, Heim CE, Xi X, et al. Monocyte metabolic reprogramming promotes pro-inflammatory activity and *Staphylococcus aureus* biofilm clearance. *PLoS Pathog*. 2020;16(3):e1008354. doi:10.1371/journal.ppat.1008354
56. Wu X, Pan B, Chu C, et al. CXCL16/CXCR6/TGF-beta feedback loop between M-MDSCs and treg inhibits anti-bacterial immunity during biofilm infection. *Adv Sci*. 2025;12(7):e2409537. doi:10.1002/advs.202409537
57. Bertol BC, Bales ES, Calhoun JD, et al. Lenvatinib plus Anti-PD-1 combination therapy for advanced cancers: defining mechanisms of resistance in an inducible transgenic model of thyroid cancer. *Thyroid*. 2022;32(2):153–163. doi:10.1089/thy.2021.0371
58. Palan J, Nolan C, Sarantos K, et al. Culture-negative periprosthetic joint infections. *EFORT Open Rev*. 2019;4(10):585–594. doi:10.1302/2058-5241.4.180067
59. Watanabe S, Kobayashi N, Tomoyama A, et al. Clinical characteristics and risk factors for culture-negative periprosthetic joint infections. *J Orthop Surg Res*. 2021;16(1):292. doi:10.1186/s13018-021-02450-1
60. Arvieux C, Common H. New diagnostic tools for prosthetic joint infection. *Orthop Traumatol Surg Res*. 2019;105(1S):S23–S30. doi:10.1016/j.otsr.2018.04.029
61. Portillo ME, Sancho I. Advances in the microbiological diagnosis of prosthetic joint infections. *Diagnostics*. 2023;13(4). doi:10.3390/diagnostics13040809
62. Scuderi GR, Mansour E, Mont MA. Diagnosing periprosthetic joint infection remains an ongoing challenge. *J Arthroplasty*. 2024;39(8):1917–1918. doi:10.1016/j.arth.2024.06.010
63. Lee YS, Koo KH, Kim HJ, et al. Synovial fluid biomarkers for the diagnosis of periprosthetic joint infection: a systematic review and meta-analysis. *J Bone Joint Surg Am*. 2017;99(24):2077–2084. doi:10.2106/JBJS.17.00123
64. Shahi A, Parvizi J. The role of biomarkers in the diagnosis of periprosthetic joint infection. *EFORT Open Rev*. 2016;1(7):275–278. doi:10.1302/2058-5241.1.160019
65. Chen MF, Chang CH, Yang LY, et al. Synovial fluid interleukin-16, interleukin-18, and CRELD2 as novel biomarkers of prosthetic joint infections. *Bone Joint Res*. 2019;8(4):179–188. doi:10.1302/2046-3758.84.BJR-2018-0291.R1
66. Saleh A, George J, Faour M, et al. Serum biomarkers in periprosthetic joint infections. *Bone Joint Res*. 2018;7(1):85–93. doi:10.1302/2046-3758.71.BJR-2017-0323
67. Prince N, Penatzer JA, Dietz MJ, et al. Localized cytokine responses to total knee arthroplasty and total knee revision complications. *J Transl Med*. 2020;18(1):330. doi:10.1186/s12967-020-02510-w

Infection and Drug Resistance

Dovepress
Taylor & Francis Group

Publish your work in this journal

Infection and Drug Resistance is an international, peer-reviewed open-access journal that focuses on the optimal treatment of infection (bacterial, fungal and viral) and the development and institution of preventive strategies to minimize the development and spread of resistance. The journal is specifically concerned with the epidemiology of antibiotic resistance and the mechanisms of resistance development and diffusion in both hospitals and the community. The manuscript management system is completely online and includes a very quick and fair peer-review system, which is all easy to use. Visit http://www.dovepress.com/testimonials.php to read real quotes from published authors.

Submit your manuscript here: https://www.dovepress.com/infection-and-drug-resistance-journal